

**MINISTRY OF EDUCATION  
AND TRAINING**

**VIETNAM ACADEMY OF SCIENCE  
AND TECHNOLOGY**

**GRADUATE UNIVERSITY OF SCIENCE AND TECHNOLOGY**



**Nguyen Thi Kim Ngan**

**FABRICATION OF PASTE CARBON ELECTRODES  
MODIFIED WITH MOF–FeBTC, MOF–CuBTC AND  
THEIR APPLICATION IN THE ANALYSIS OF  
AMOXICILLIN AND ENROFLOXACIN  
IN SURFACE WATER**

**SUMMARY OF DISSERTATION ON SCIENCES OF MATTER**

**Major: Analytical chemistry**

**Code: 9 44 01 18**

**HA NOI, 2025**

The dissertation is completed at: Graduate University of Science and Technology, Vietnam Academy Science and Technology

Supervisors:

1. Supervisor 1: PhD.Pham Thi Hai Yen
2. Supervisor 2: Assoc.Prof. Vu Thi Thu Ha

Referee 1: .....

Referee 2: .....

Referee 3: .....

The dissertation is examined by Examination Board of Graduate University of Science and Technology, Vietnam Academy of Science and Technology at.....

The dissertation can be found at:

1. Graduate University of Science and Technology Library
2. National Library of Vietnam

## LIST OF THE PUBLICATIONS RELATED TO THE DISSERTATION

1. **Thi Kim Ngan Nguyen**, Tien Hung Nguyen, Manh B. Nguyen, Hoang Anh Nguyen, Thi Thu Ha Vu, Quoc Hung Le, Quang Hai Tran, and Thi Hai Yen Pham, Synthesis of Nanostructured Mixed-Valence Fe(II,III) Metal- Organic Framework and Its Application in Electrochemical Sensing of Amoxicillin, *Journal of The Electrochemical Society*, 2023 170 056505  
Doi: 10.1149/1945-7111/acced6
2. **Nguyen Thi Kim Ngan**, Tien Dat Doan, Luu Huy Hieu, Nguyen Hoang Anh, Thi Thu Ha Vu, Quang Hai Tran, Ha Tran Nguyen, Thanh Binh Dang, Thi Hai Yen Pham, and Mai Ha Hoang, Electrochemical nanocstructured CuBTC/FeBTC MOF composite sensor for enrofloxacin detection, *Beilstein Journal of nanotechnology* **2024**, 15, 1522 – 1535  
<https://doi.org/10.3762/bjnano.15.120>
3. Doan Tien Dat, Pham Thi Hai Yen, **Nguyen Thi Kim Ngan**, Doan Tat Dat, Tran Quang Hai, Hac Thi Nhung, Ho Thi Oanh, Nguyen Duc Tuyen, Le Quoc Hung, Vu Thi Thu Ha, Le Thu Thao, Hoang Van Hung, Hoang Mai Ha, Fabrication of CuBTC and FeBTC metal-organic frameworks for highly sensitive and selective simulateous detection of amoxicillin and enrofloxacin, *Journal of chemistry and application- 3B( 71)- 9/2024*

## INTRODUCTION

Since their discovery in 1928, antibiotics have saved millions of lives. However, their overuse, particularly in livestock farming, has led to environmental residues and the rise of antibiotic-resistant bacteria. Vietnam is among the countries with the highest antibiotic resistance rates. Residues of antibiotics such as amoxicillin and enrofloxacin have been detected in wastewater, surface water, and drinking water, even though enrofloxacin has been banned in several countries.

Modern analytical techniques such as HPLC, LC-MS, and GC-MS offer high accuracy but are costly, complex, and challenging to implement in field conditions. In contrast, electrochemical methods are simple, cost-effective, and allow for rapid on-site analysis. Metal-organic frameworks (MOFs), particularly MOF–FeBTC and MOF–CuBTC, have emerged as promising materials for electrochemical sensors due to their high surface area and strong interaction capabilities, enhancing the sensitivity and selectivity of amoxicillin (AMX) and enrofloxacin (ENR) detection.

To build upon and advance research on the application of advanced materials for electrode modification in antibiotic determination in environmental samples, this dissertation presents a novel study aimed at developing MOF–FeBTC- and MOF–CuBTC-based electrodes for the electrochemical analysis of amoxicillin and enrofloxacin. The research is titled: **"Fabrication of Paste Carbon Electrodes Modified with MOF–FeBTC, MOF–CuBTC and Their Application in the Analysis of Amoxicillin and Enrofloxacin in Surface Water."** This study seeks to enhance the sensitivity and selectivity of electrochemical analysis, thereby improving the detection of amoxicillin and enrofloxacin residues in environmental samples.

## Research Objectives

This dissertation aims to develop MOF-modified paste carbon electrodes (CPEs) using Cu and Fe metal centers with trimesic acid (BTC) ligands for the sensitive and selective electrochemical detection of amoxicillin and enrofloxacin in water samples.

Key tasks include:

- Synthesizing and characterizing MOFs;
- Fabricating and evaluating MOF-modified CPEs;
- Assessing their application in antibiotic detection.

## Scientific and Practical Significance

The study develops a highly sensitive electrochemical sensor for detecting enrofloxacin (banned) and amoxicillin (widely used), aiding pollution control. MOF-modified electrodes (CuBTC, FeBTC) enhance sensitivity, reproducibility, and detection limits, enabling trace-level analysis.

## Novel Contributions of the Dissertation

1. Successfully applied the FeBTC-modified paste carbon electrode (FeBTC)CPE for the determination of amoxicillin in tap water and water samples from West Lake. The method exhibited high sensitivity, achieving a low detection limit of 0.107  $\mu\text{M}$ .
2. Applied CuBTC-modified paste carbon electrode (CuBTC)CPE and (CuBTC)(FeBTC)CPE for the determination of enrofloxacin. The (CuBTC)(FeBTC)CPE demonstrated superior analytical performance, achieving an ultra-low detection limit of 3.00 nM.
3. Successfully employed the mixed (CuBTC)(FeBTC)CPE electrode for the simultaneous electrochemical analysis of amoxicillin and enrofloxacin in water. Optimal analytical conditions were established for the effective simultaneous determination of both antibiotics.

excellent selectivity, and reliable quantification of AMX in tap water and West Lake water samples, yielding recoveries of 101.5% and 109%, respectively.

3. The (CuBTC)CPE with a 10% w/w CuBTC content and the hybrid (CuBTC)(FeBTC)CPE with a CuBTC:FeBTC ratio of 5:5 (% w/w) were employed for the electrochemical analysis of enrofloxacin in aqueous solutions. Under optimized conditions (0.1 M PBS buffer, pH = 7.0), the hybrid (CuBTC)(FeBTC)CPE exhibited superior analytical performance compared to the (CuBTC)CPE, offering three distinct linear concentration ranges: 0.005–0.10  $\mu\text{M}$ , 0.1–1.0  $\mu\text{M}$ , and 1.0–13.0  $\mu\text{M}$ . Both electrodes provided high reproducibility (RSD = 4.5% and 3.83%), excellent selectivity, and accurate ENR determination in tap water and West Lake water samples, with recoveries ranging from 91% to 110%. The hybrid (CuBTC)(FeBTC)CPE achieved an LOD of 3.0 nM and a sensitivity of 56.1  $\mu\text{A}/\mu\text{M}$ .
4. The simultaneous determination of ENR and AMX was successfully demonstrated using the hybrid (CuBTC)(FeBTC)CPE. The optimal MOF composition was determined to be CuBTC:FeBTC (% w/w) = 5:10. Under optimized conditions (0.1 M PBS buffer, pH = 10, adsorption time = 60 s), well-separated peaks for AMX and ENR were obtained ( $\Delta E = 0.21\text{ V}$ ). The electrode exhibited a good linear response in the concentration ranges of 20–80  $\mu\text{M}$  for AMX and 0.2–0.8  $\mu\text{M}$  for ENR, with LODs of 5.24  $\mu\text{M}$  and 0.03  $\mu\text{M}$  for AMX and ENR, respectively.

## CONCLUSION

Based on the obtained results from the research conducted in this dissertation, the following conclusions can be drawn:

1. Metal–organic frameworks (MOFs) including CuBTC and FeBTC were successfully synthesized using the solvothermal method. The MOF–FeBTC material was found to contain both  $\text{Fe}^{2+}$  and  $\text{Fe}^{3+}$  oxidation states, indicating the coexistence of mixed-valence iron centers. The MOF–CuBTC exhibited a well-defined cubic structure with relatively large particle sizes. MOF-modified electrodes were prepared by incorporating the synthesized materials into a carbon paste electrode (CPE) matrix, resulting in uniform and homogeneous electrode surfaces. The (FeBTC)CPE electrode demonstrated superior charge transfer properties compared to the unmodified (bare) CPE, while the (CuBTC)CPE electrode exhibited excellent adsorption capacity toward the target analyte. Notably, the composite electrode (CuBTC)(FeBTC)CPE displayed a synergistic effect between the two MOFs, leading to enhanced charge transfer efficiency and significantly improved electrochemical signal response.
2. The (FeBTC)CPE, with an optimal FeBTC loading of 5% w/w, was effectively employed for the electrochemical determination of amoxicillin in water. This electrode offered advantages such as simple fabrication, good reproducibility, and stability in low-pH environments. Under optimal analytical conditions (0.1 M PBS buffer, pH = 3, adsorption time = 120 s), the electrode exhibited a well-defined linear relationship in the concentration range of 1.0–100.0  $\mu\text{M}$  with a limit of detection (LOD) of 0.107  $\mu\text{M}$ . The method demonstrated high reproducibility (RSD = 4.88%),

## CHAPTER 1: LITERATURE REVIEW

This section reviews amoxicillin (AMX) and enrofloxacin (ENR), their health risks, and antibiotic contamination in water and food. It summarizes antibiotic detection methods, focusing on chromatography and electrochemical techniques, and explores electrode modifications using nanocarbon, metals, oxides, polymers, and MOFs. Research on electrochemical antibiotic analysis in Vietnam and globally is also highlighted.

## CHAPTER 2: EXPERIMENTAL

The 12-page document details the synthesis of MOF–CuBTC and MOF–FeBTC, modification of carbon paste electrodes (CPE), and fabrication of modified electrodes. It covers material and electrode surface characterization using XRD, SEM, TEM, EDX, XPS, FT-IR, and BET for MOF–CuBTC, MOF–FeBTC, and modified electrodes (FeBTC)CPE, (CuBTC)CPE, and (CuBTC)(FeBTC)CPE. It also explores optimization conditions for antibiotic (AMX, ENR) analysis, including material ratio, electrolyte composition, pH, and adsorption time, as well as simultaneous detection. Additionally, it describes real water sample collection and sensor performance evaluation, including repeatability, reproducibility, calibration, and selectivity.

## CHAPTER 3: RESULTS AND DISCUSSION

### 3.1. Properties of MOF Materials

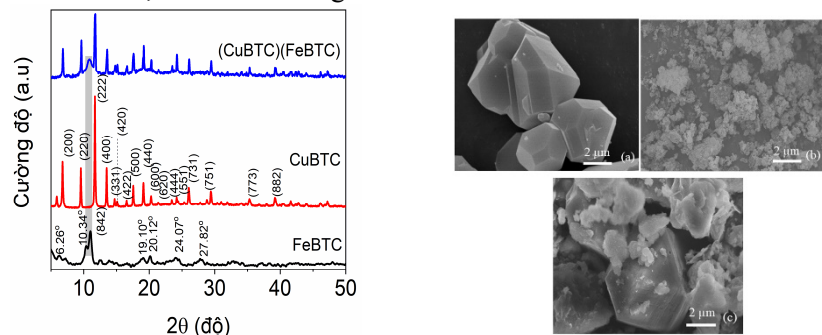
#### + *Crystalline Characteristics of MOFs*

Figure 3.1 presents the XRD patterns of the synthesized MOF materials. The characteristic peaks of MOF–FeBTC appear at  $2\theta$  values of approximately 4.10°, 6.13°, 10.26°, 10.85°, 19.10°, 24.07°, and 27.82°, with a distinctive peak at 11.91° indicating the specific structure of the material. Meanwhile, the characteristic peaks of MOF–CuBTC are

observed at  $6.77^\circ$ ,  $9.65^\circ$ ,  $11.73^\circ$ , and  $14.76^\circ$ , confirming its cubic crystalline structure

#### + Morphological Characteristics of MOFs

The synthesized MOF–FeBTC exhibits a morphology resembling small spherical particles with a relatively uniform distribution, while MOF–CuBTC adopts a cubic structure with particle sizes of several tens of nanometers, as shown in Figure 3.1.



**Figure 3.1. XRD Patterns and Corresponding SEM Images of Modified Materials: CuBTC (a), FeBTC (b), and the CuBTC-FeBTC Composite (c)**

#### + Chemical Structural Characterization of MOF Materials

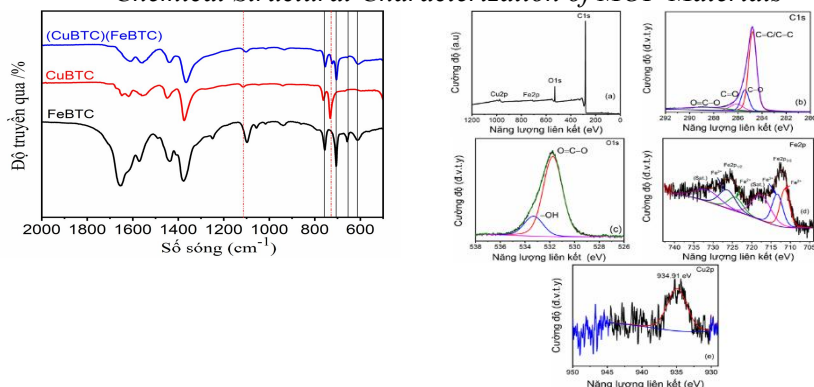


**Figure 3. 2.FT-IR spectra of the materials and XPS spectra of the (CuBTC)(FeBTC)**

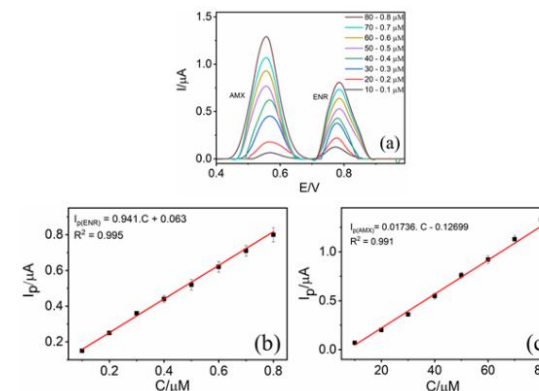


**Figure 3.12. SW-AdSV of the (CuBTC)(FeBTC)CPE electrode for the simultaneous measurement of AMX and ENR signals at different concentrations, along with the plot showing the relationship between the concentration of AMX (b) and ENR (c) and the peak current ( $I_p$ ).**

**Table 3.5. Evaluation of the simultaneous analysis method for AMX and ENR using the modified (CuBTC)(FeBTC)CPE electrode.**

Parameter	AMX	ENR
Working range	Working range 20 – 80 $\mu\text{M}$	Working range 0.2 – 0.8 $\mu\text{M}$
Calibration curve	Calibration curve $y = 0.017 \cdot x - 0.127$	Calibration curve $y = 0.941 \cdot x + 0.063$
LOD ( $\mu\text{M}$ )	5.4	0.03
LOQ ( $\mu\text{M}$ )	17.29	0.099

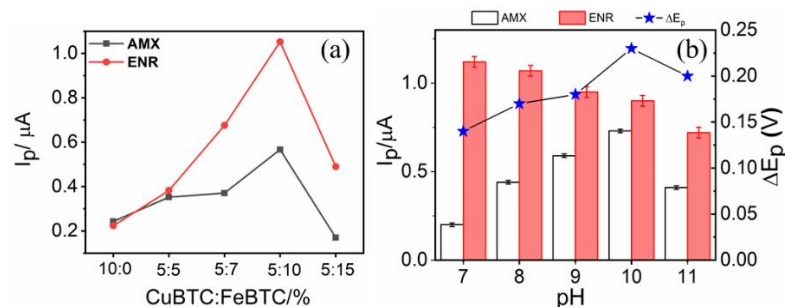


**Figure 3.11. SW-AdSV of AMX and ENR at different pH values (a) and the graph showing the relationship between peak height of AMX and ENR as a function of pH and  $E_p$  (b).**

+ Adsorption Time Optimization

The adsorption time  $t_{acc}=60s$  was selected as the optimal condition for this analysis.

+ Calibration Curve, Limit of Detection, and Limit of Quantification

The linear regression equations for AMX and ENR analysis are:

- **For AMX:**  $y = 0.017 \cdot x - 0.127$  ( $R^2 = 0.995$ )
- **For ENR :**  $y = 0.94 \cdot x + 0.063$  ( $R^2 = 0.994$ )

The electrode exhibited good linear correlation within the concentration range of **20.0  $\mu M$  to 80.0  $\mu M$**  for AMX with an LOD of **5.24  $\mu M$** , and **0.2  $\mu M$  to 0.8  $\mu M$**  for ENR with an LOD of **0.03  $\mu M$** .

The FT-IR spectrum of the MOF material (Figure 3.2a) exhibits characteristic vibrational bands at  $666 \text{ cm}^{-1}$  and  $612 \text{ cm}^{-1}$ , which correspond to Fe–O,  $\text{Fe}_3\text{O}_4$ , and C–O–Fe bonds. Additionally, the vibrational band at  $1109 \text{ cm}^{-1}$  is attributed to the stretching mode of the C–O–Cu bond, while the bands at  $730 \text{ cm}^{-1}$  and  $760 \text{ cm}^{-1}$  are characteristic of the C–O–Cu linkage in the CuBTC material.

The XPS spectrum of the (CuBTC)(FeBTC) composite, as shown in Figure 3.2b, reveals two sets of binding states, represented by split peaks at approximately 713.0 eV and 726.0 eV. A more detailed peak analysis indicates that the peaks at 711.30 eV and 714.12 eV correspond to  $\text{Fe}^{2+}$  and  $\text{Fe}^{3+}$  species, respectively, which are consistent with the binding energy of the Fe  $2p_{3/2}$  orbital. Similarly, the Fe  $2p_{1/2}$  peaks at 724.90 eV and 727.72 eV further confirm the presence of  $\text{Fe}^{2+}$  and  $\text{Fe}^{3+}$  ions. These findings suggest that the FeBTC MOF exhibits mixed-valence characteristics. In the case of CuBTC, the binding energy at 934.91 eV is assigned to  $\text{Cu}^{2+}$  ions within the composite structure

+ Porosity characteristics, surface area

**Bảng 3.1: Characteristic Parameters of the Modified Materials**

	MOF material	Surface area $\text{m}^2/\text{g}$	Pore volume $\text{cm}^3/\text{g}$	Pore diameter nm
1	FeBTC	1211	1,46	2,38
2	CuBTC	1134	0,49	1,74
3	(CuBTC)(FeBTC)	1147	0,544	1,50

**3.2. Electrochemical Properties of the Modified Electrodes (FeBTC)CPE, (CuBTC)CPE, and (CuBTC)(FeBTC)CPE**

+ Cyclic Voltammetry (CV)

Cyclic voltammetry scans reveal that the (FeBTC)CPE electrode exhibits a well-defined  $\text{Fe}^{3+}/\text{Fe}^{2+}$  redox couple, sharper than that observed for the bare electrode. This indicates an increased electroactive surface area

and enhanced charge transfer kinetics, attributed to the presence of FeBTC with  $\text{Fe}^{3+}/\text{Fe}^{2+}$  redox sites.

For the (CuBTC)CPE and (CuBTC)(FeBTC)CPE electrodes, in addition to the  $\text{Fe}^{3+}/\text{Fe}^{2+}$  redox couple, oxidation peaks corresponding to Cu oxidation processes appear at 0.1 V, -0.16 V, and 0.03 V. These peaks are associated with the Cu redox transitions, enabling the electrode to operate at potentials more positive than 0.2 V without compromising the stability of the MOF structures within the electrode.

#### + Electrochemical Impedance Spectroscopy (EIS)

The charge transfer resistance ( $R_{ct}$ ) values for the modified electrodes (FeBTC)CPE, (CuBTC)CPE, (CuBTC)(FeBTC)CPE were measured as 623  $\Omega$ , 220  $\Omega$ , 1510  $\Omega$ , and 547  $\Omega$ , respectively.

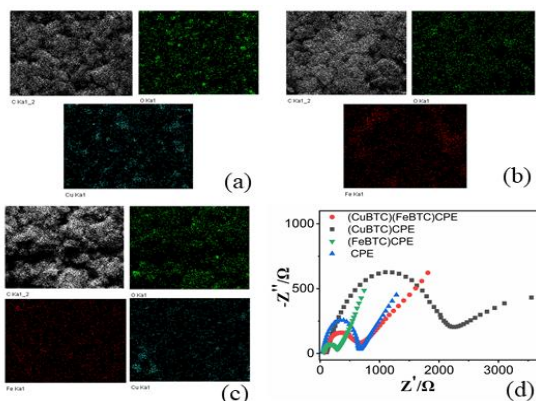


**Figure 3.3**  
**EDX-mapping of**  
**(CuBTC)CPE (a),**  
**(FeBTC)CPE (b),**  
**(CuBTC)(FeBTC)CPE**  
**(c) electrode and EIS**  
**of the electrodes**

#### EDX mapping

The electrode fabricated using the blending method exhibits high uniformity, ensuring stability and enhancing the reproducibility of the analytical measurement signals.

### 3.3. Analysis of AMX Using the Modified (FeBTC)CPE Electrode

+ Electrochemical Properties of AMX on the (FeBTC)CPE Electrode

(CuBTC)(FeBTC)CPE electrode was 44 times higher than that of the bare CPE and twice that of the (CuBTC)CPE electrode. Additionally, the peak-to-peak potential separation ( $\Delta E$ ) was the largest at 0.21 V.

The simultaneous detection of AMX and ENR using the modified electrodes, as shown in Figure 3.10, confirms that the (CuBTC)(FeBTC)CPE electrode is suitable for the simultaneous determination of AMX and ENR in solution.

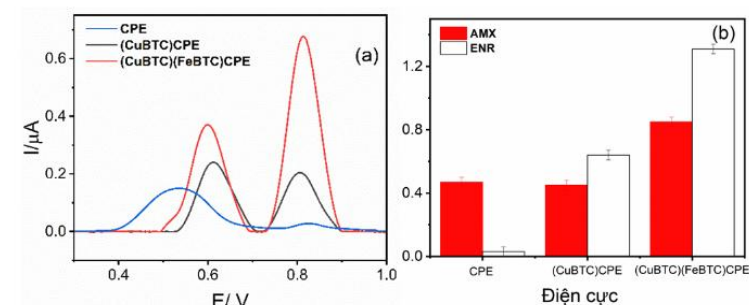


**Figure 3.10: SW-AdSV of AMX and ENR under the same conditions with AMX concentration of 50.0  $\mu\text{M}$  and ENR concentration of 0.40  $\mu\text{M}$ .**

#### + Investigation of MOFs composition

When fixing the CuBTC content at 5% and varying the FeBTC content, the results indicated that a CuBTC:FeBTC ratio of 5:15 provided the best analytical signals for AMX and ENR (Figure 3.11a).

#### + Investigation of pH for simultaneous analysis of AMX and ENR

PBS solution was used as the electrolyte medium for the simultaneous determination of AMX and ENR. A pH of 10.0 was selected as the optimal condition, as it allowed for the best simultaneous detection of AMX and ENR signals while minimizing peak interference.



water. These recovery values are considered acceptable for analyte concentrations in the  $\mu\text{M}$  range, confirming the accuracy of the electrochemical method using the fabricated modified electrodes.

Further validation was performed by analyzing the spiked ENR samples using **LC-MS/MS** as a reference method. The ENR concentrations determined by the electrochemical method were in good agreement with the LC-MS/MS results, with a low deviation of **8.0%**, further confirming the accuracy of the developed sensor.

**Table 3.3. Comparison and evaluation of the ENR analysis method using modified electrodes (CuBTC)CPE and (CuBTC)(FeBTC)CPE**

Parameter	(CuBTC)CPE	(CuBTC)(FeBTC)CPE
<b>Working range</b>	Working range 0.01–12.0 $\mu\text{M}$	Working range 0.005 – 13.0 $\mu\text{M}$
<b>Linear range</b>	- 3 linear range: 0.01 – 0.15 $\mu\text{M}$ ; 0.1 – 2.0 $\mu\text{M}$ ; 1.0 – 12.0 $\mu\text{M}$	- 3 linear range: 0.005 – 0.1 $\mu\text{M}$ ; 0.1 – 1.0 $\mu\text{M}$ ; 1.0 – 13.0 $\mu\text{M}$
<b>RSD</b>	4.5%	3.83%
<b>Sensitive</b>	33.3 $\mu\text{A}/\mu\text{M}$	56.1 $\mu\text{A}/\mu\text{M}$
<b>LOD</b>	9.0 nM	3.0 nM
<b>LOQ</b>	29.7 nM	9.9 nM
<b>Recovery</b>	96.5% - 103.0%	91.0 % - 110.0%

### 3.5. Simultaneous analysis of AMX and ENR using the modified electrode (CuBTC)(FeBTC)CPE

#### + Electrochemical Property Investigation

The individual electrochemical responses of AMX (50  $\mu\text{M}$ ) and ENR (0.4  $\mu\text{M}$ ) were evaluated using CPE, (CuBTC)CPE, and (CuBTC)(FeBTC)CPE electrodes. The results demonstrated that the modified electrode incorporating both MOFs exhibited the highest signal intensities. Specifically, for AMX, the peak current ( $I_p$ ) recorded with the (CuBTC)(FeBTC)CPE electrode was twice as high as that obtained with CPE and (CuBTC)CPE. For ENR, the  $I_p$  value on the

The electrochemical response of AMX on the modified electrode was investigated using cyclic voltammetry (CV) and square wave adsorptive stripping voltammetry (SW-AdSV) in AMX solutions of 200  $\mu\text{M}$  and 40.00  $\mu\text{M}$  in PBS buffer at pH 7. The results revealed a single oxidation peak at 0.75 V, which is more negative compared to the oxidation peak of AMX observed on the unmodified CPE electrode. This shift indicates that FeBTC effectively facilitates the oxidation of AMX, enhancing the electrochemical reaction kinetics.

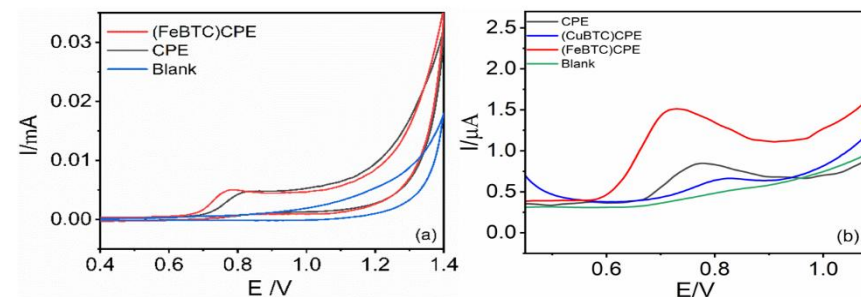


**Figure 3.4. CV and SW-AdSV Analysis of the CPE and Modified Electrodes in AMX/PBS Solution**

#### + Optimization of Electrode Composition

The study on the composition ratio of the modified electrode revealed that an MOF–FeBTC content of 5% (w/w) produced the highest AMX signal (Figure 3.5a), with a well-defined and symmetric oxidation peak. This can be attributed to the excellent electrocatalytic activity and good electrical conductivity of FeBTC. Therefore, a 5% FeBTC loading was selected as the optimal condition for subsequent studies.

#### + Investigation of Supporting Electrolyte Composition and pH Effects

PBS buffer at pH 3 (Figure 3.5b) was identified as the most suitable supporting electrolyte for further studies. At pH 3, AMX predominantly exists in its zwitterionic form ( $\text{AMX}^\pm$ ), while the electrode surface carries a

negative charge. This charge interaction facilitates the electrochemical oxidation process, leading to enhanced analytical performance.

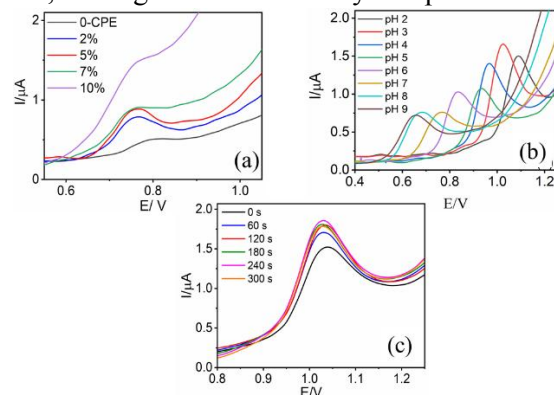


**Figure 3. 5. Optimization of Experimental Conditions: FeBTC Ratio (a), pH (b), and Adsorption Time (c))**

#### + Adsorption Time Investigation

The optimal adsorption time ( $t_{acc}$ ) was set at 120 seconds as the optimal  $t_{acc}$  for further studies.

#### Evaluation of Sensor Performance

##### + Reproducibility and Repeatability

The repeatability test, conducted over five consecutive measurements of the AMX signal on the same electrode, showed a gradual decrease in signal intensity, indicating that the electrode surface needs to be refreshed after each measurement.

For the reproducibility assessment, nine repeated measurements under optimal conditions yielded a relative standard deviation (RSD%) of **4.88%**, demonstrating good repeatability of the sensor.

##### + Calibration Curve, Limit of Detection (LOD), and Limit of Quantification (LOQ)

In the AMX concentration range of **0 – 100  $\mu\text{M}$** , the peak current exhibited a linear dependence on the AMX concentration, following the equation:  $y=0.024x + 0.0059$  ( $R^2 = 0.9985$ )

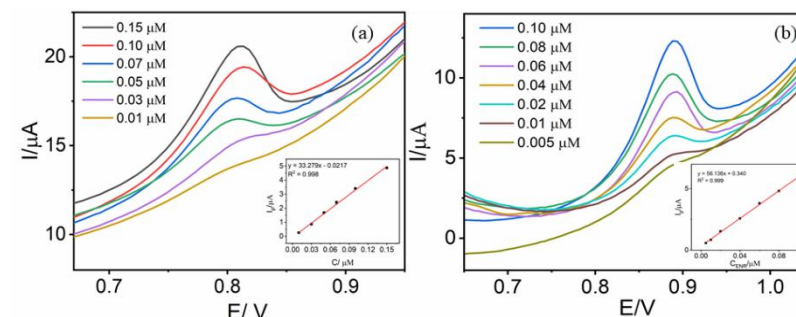


**Figure 3.9. SW-AdSV Response of ENR at the Lowest Calibration Concentration**

**For (CuBTC)(FeBTC)CPE:** The electrochemical response of ENR exhibited linearity over three concentration ranges

$$\mathbf{0.01 - 0.15 \mu M: } y=56.136*x+0.340 \text{ (} R^2=0.9990 \text{)}$$

$$\mathbf{0.1 - 2.0 \mu M: } y=11.373*x-0.128 \text{ (} R^2=0.9953 \text{)}$$

$$\mathbf{1.0 - 13.0 \mu M: } y=1.225x-0.557 \text{ (} R^2=0.9992 \text{)}$$

LOD and LOQ were determined to be **3.00 nM** and **9.90 nM**, respectively, with a sensitivity of **56.1  $\mu\text{A}/\mu\text{M}$** .

#### + Selectivity of the Method

The ENR signal on (CuBTC)CPE and (CuBTC)(FeBTC)CPE remained largely unchanged in the presence of inorganic ions ( $\text{Na}^+$ ,  $\text{K}^+$ ,  $\text{Ca}^{2+}$ ,  $\text{Zn}^{2+}$ ,  $\text{Fe}^{2+}$ ,  $\text{Ni}^{2+}$ ,  $\text{Pb}^{2+}$ ,  $\text{NH}_4^+$ ,  $\text{Cu}^{2+}$ ,  $\text{NO}_3^-$ ,  $\text{SO}_4^{2+}$ ,  $\text{Cl}^-$ ) at 100-fold higher concentrations and organic compounds (PA, CAP, ERY, AA, DA, PA, GLU, OXA, oxytetracycline, CEF, AMX) at 10- and 50-fold higher concentrations. However, interfering substances should be removed prior to sample analysis to ensure accuracy

#### + Real Sample Analysis and Accuracy Evaluation of the Method

ENR was not detected in the collected tap water and West Lake water samples. Standard addition experiments were conducted by spiking the samples with **0.2  $\mu\text{M}$**  ENR, followed by analysis using the developed method. The recovery rates obtained for each modified electrode ranged from **96.5% to 114.5%** for tap water and **97.3% to 110.6%** for West Lake

**For (CuBTC)CPE:** The optimal adsorption time ( $t_{acc}$ ) varied with ENR concentration. At lower concentrations, longer  $t_{acc}$  was required, while at higher concentrations, shorter  $t_{acc}$  was sufficient. The selected  $t_{acc}$  values for different concentration ranges were 0 s, 180 s, and 300 s.

**For (CuBTC)(FeBTC)CPE:** Similarly, the optimal  $t_{acc}$  varied with ENR concentration. The selected  $t_{acc}$  values were 0 s, 90 s, and 600 s.

#### *Sensor Performance Evaluation*

##### *+ Repeatability and Reproducibility*

The electrochemical response of ENR was evaluated through five consecutive measurements using (CuBTC)CPE and (CuBTC)(FeBTC)CPE. A gradual decrease in signal intensity was observed, indicating the need for electrode surface renewal after each measurement. Under optimal conditions, the relative standard deviations (RSD%) for ENR signals obtained from (CuBTC)CPE and (CuBTC)(FeBTC)CPE were 4.5% and 3.83%, respectively, demonstrating good repeatability

##### *+ Calibration Curve – Limit of Detection (LOD) – Limit of Quantification (LOQ)*

- **For (CuBTC)CPE:** The electrochemical response of ENR exhibited linearity over three concentration ranges:  
**0.01 – 0.15  $\mu\text{M}$ :**  $y=0.024x+0.0059$  ( $R^2=0.9984$ )  
**0.1 – 2.0  $\mu\text{M}$ :**  $y=8.497x+0.356$  ( $R^2=0.9984$ )  
**2.0 – 12.0  $\mu\text{M}$ :**  $y=0.7502x+0.1375$  ( $R^2=0.9977$ )

The LOD and LOQ values for (CuBTC)CPE were determined to be **9.00 nM** and **29.7 nM**, respectively, with a sensitivity of **33.3  $\mu\text{A}/\mu\text{M}$** .

The **LOD** and **LOQ** were determined to be **0.107  $\mu\text{M}$**  and **0.353  $\mu\text{M}$** , respectively. The sensor exhibited a sensitivity of **25.38  $\mu\text{A}/\mu\text{M}$** , indicating its high analytical performance.

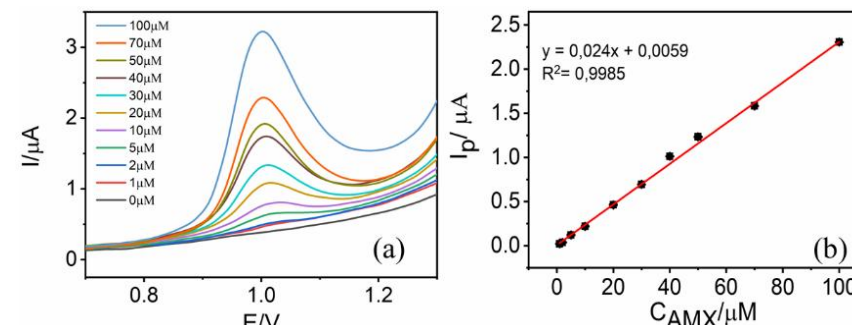


**Figure 3. 6 SW-AdSV response of AMX at different concentrations from 1.00 to 100  $\mu\text{M}$  (a) and the calibration curve showing the relationship between AMX concentration and peak height (b)**

##### *+ Selectivity of the Method*

The AMX signal on the (FeBTC)CPE electrode remained nearly unchanged in the presence of inorganic ions ( $\text{Na}^+$ ,  $\text{K}^+$ ,  $\text{Ca}^{2+}$ ,  $\text{Mg}^{2+}$ ,  $\text{Zn}^{2+}$ ,  $\text{Ni}^{2+}$ ,  $\text{NH}_4^+$ ,  $\text{NO}_3^-$ ,  $\text{SO}_4^{2-}$ ,  $\text{Cl}^-$ ,  $\text{HCO}_3^-$ ) at concentrations 100 times higher, as well as organic compounds (ascorbic acid, dopamine, glucose, paracetamol, chloramphenicol, and the sodium salt of uric acid) at concentrations 10 and 50 times higher. These results confirm that the electrochemical method using the (FeBTC)CPE electrode exhibits excellent selectivity for AMX detection.

##### *+ Antibiotic Analysis in Real Samples and Method Comparison*

AMX was not detected in the collected tap water and West Lake water samples. Spiked samples with **5.0  $\mu\text{M}$**  AMX were analyzed using the standard addition method, yielding recovery rates of **101.5%** for tap water and **109%** for West Lake water. These recovery values are acceptable for analyte concentrations in the micromolar range, confirming the accuracy of the analysis using the fabricated modified electrode.

Comparative analysis of AMX-spiked samples using the reference LC/MS-MS method showed that the AMX concentrations obtained by the electrochemical method were consistent with the reference results. The measurement discrepancy between the two methods was low, with an error of **2.10%**, demonstrating the reliability of the electrochemical approach.

**Table 3.2. Evaluation of AMX analysis using the modified electrode (FeBTC)CPE**

Parameter	(FeBTC)CPE
Working Range	Working range 1.0 – 100 $\mu\text{M}$
Calibration curve	Calibration curve $y = 0.024 \cdot x + 0.0059$
RSD	4.5%
LOD	0.107 $\mu\text{M}$
LOQ	0.353 $\mu\text{M}$
Độ nhạy	25.38 $\mu\text{A}/\mu\text{M}$
Độ thu hồi	101.5% - 109.0%

### 3.4. ENR analysis using modified electrodes (CuBTC)CPE and (CuBTC)(FeBTC)CPE

#### + Electrochemical properties of ENR on the modified electrode

The electrochemical response of ENR on the modified (CuBTC)CPE and (CuBTC)(FeBTC)CPE electrodes was investigated using CV and SW-AdSV techniques in **200  $\mu\text{M}$**  and **0.5  $\mu\text{M}$**  ENR solutions prepared in PBS (**pH = 7**). A single oxidation peak was observed at **0.88 V**, which is more negative than the oxidation peak of ENR on the unmodified CPE electrode. This indicates that **CuBTC** and **FeBTC** enhance the catalytic activity for the oxidation of ENR.

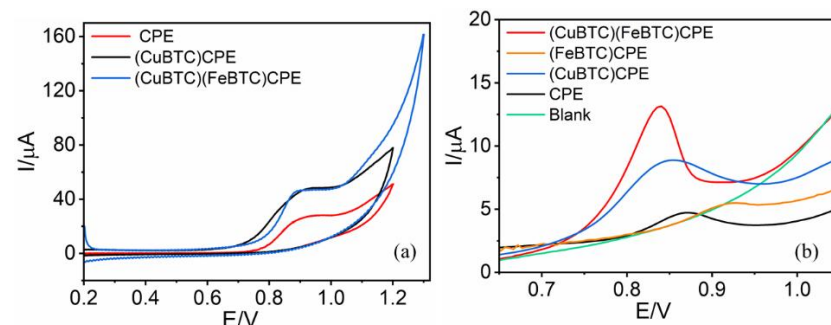


**Figure 3. 7. CV of the CPE and the modified electrodes (a), SWAd-SV of the CPE and the modified electrodes in ENR/PBS solution**

#### + Investigation of Electrode Composition Ratio

The %w/w ratios of **CuBTC** and the **CuBTC:FeBTC** mixture in the modified electrodes were determined as **10%** and **5:5%**, respectively, as shown in **Figure 3.8a,b**. These ratios were identified as optimal for subsequent studies.

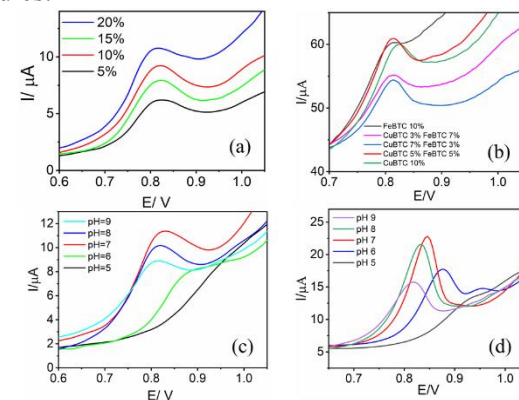


**Figure 3.8. SWAd-SV of 0.5  $\mu\text{M}$  ENR/PBS with different CuBTC (a), CuBTC:FeBTC (b) Ratios and pH Values (c, d)**

#### + Investigation of Electrolyte Composition – pH of the Electrolyte Solution

A 0.1 M PBS solution at pH 7 was selected as the optimal electrolyte for subsequent studies

#### + Adsorption Time Optimization